Kinematics and Dynamics Optimization of a Novel Non-circular Gear-attached Four-bar Mechanism for Knee Exoskeleton Robot

Hojjat Sabzali
Mechanical Engineering Department, Center of Advance Rehabilitation and Robotic Research (FUM-CARE)
Ferdowsi University of Mashhad
Mashhad, Iran
hsabzali@mail.um.ac.ir

Erfan Koochakzadeh
Mechanical Engineering Department, Center of Advance Rehabilitation and Robotic Research (FUM-CARE)
Ferdowsi University of Mashhad
Mashhad, Iran
erfan.koochakzadehdandansaz@mail.um.ac.ir

Ali Moradi
Orthopedic Research Center
Mashhad University of Medical Sciences
Mashhad, Iran
moradial@mums.ac.ir

Alireza Akbarzadeh
Mechanical Engineering Department, Center of Advance Rehabilitation and Robotic Research (FUM-CARE)
Ferdowsi University of Mashhad
Mashhad, Iran
ali_akbarzadeh@um.ac.ir

2022 10th RSI International Conference on Robotics and Mechatronics (ICRoM) | 978-1-6654-5452-0/22/$31.00 ©2022 IEEE | DOI: 10.1109/ICRoM57054.2022.10025342

***Abstract*— Minimizing weight and required motor torque as well as improving comfort is critical in designing exoskeletons. This paper proposes a novel non-circular gear-attached four-bar (NGF) mechanism with a J-shaped instantaneous center of rotation (ICR) for a knee exoskeleton. In this work, the ICR of the knee is classified into two distinct groups. One, is the physiological ICR, and the other is the ICR of the knee. These two ICRs were measured by fluoroscopy and motion capture of a healthy volunteer, respectively. Using a kinematic approach, the tracking error of both ICRs are minimized and the best-fitted elliptical curve for each of the ICRs is obtained. Next, the two elliptical curves are combined and a pair of non-circular gears is designed. Finally, system dynamics is considered to obtain design parameters resulting in minimum range of actuator torque while minimizing the mechanism weight.**

Keywords—Knee joint mechanism, instantaneous center of rotation, fluoroscopy, motion capture, full lunge movement, dynamics optimization, kinematics optimization

I. INTRODUCTION

Knee exoskeleton robots are wearable and rehabilitation robots. People with functional knee problems, like the elderly, knee injuries, and complications related to knee arthroplasty surgery use these robots as assistive devices. The biology motion of the human knee joint include various motions such as internal rotation, varus rotation, posterior translation and the flexion-extension rotations. All these combined result in a sliding and a gliding motion that occur simultaneously. As a result, the instantaneous center of rotation (ICR) of this joint is J-shaped in sagittal plane [1]. The Femur and Tibia have different relative transitional distances in knee flexion and extension [2]. If the robot's mechanism does not strictly follow the ICR of the knee, it will cause additional force in the robot fasteners. These potential tangential forces cause the robot to move and slip in the locations of the fasteners [3]. Consequently, one of the considerable characteristics of knee mechanisms is to follow the ICR of the knee. In this category of robots, different mechanisms are used to track the ICR of the human knee joint. Generally, these mechanisms are categorized into two types which are uniaxial and multi-axial [4]. Some of these are described below.

In the knee joint, the four-bar mechanism is commonly used for its simplicity and good fitting of the ICR of the knee [5]. For instance, the TLBO algorithm simplifies the dimensional synthesis of the four-bar mechanism [6]. A cross four-link mechanism has been made, and its lengths have been optimized for a better fit knee ICR trajectory [7]. Knee joint bearing performance is improved by adding a rolling bearing to the four-bar mechanism [8]. Two 6-link one-degree-of-freedom mechanisms consisting of two four-link mechanisms have been presented with kinematic and dynamic optimization [9]. To improve the payload capacity of the exoskeleton, a linear actuator and a sub-link mechanism are applied to the knee joint [10]. The knee mechanism has been used by considering the cam and gear on the contact surface to move the ICR of the knee using the measured data [11]. Furthermore, a pair of gears have been added to the five-bar mechanism in order to improve the fit of the ICR of the knee joint [12]. In this paper, we consider the resulting sagittal motion of a knee and a single degree of freedom non-circular gear-attached four-bar (NGF) mechanism is introduced. The design of the non-circular gears is based on the ICR. Because the physiological ICR vastly differs from the ICR obtained from motion capture approach [13], The ICR is measured in the sagittal plan in two ways which are the fluoroscopy and motion capture in open kinematic chain (Femur is stationary) movement [14]. Finally, the design parameters of the single degree of freedom NGF mechanism are presented based on the minimum range of actuator torque and total mass of the mechanism in full lunge movement.

The rest of this paper is organized as follows. In section II, the fluoroscopy and motion capture processes are explained. In section III, the overview of our method and the optimizations are introduced, which leads to optimization results and discussion in section IV. Finally, section V concludes the paper.

II. MEASUREMENT AND CALCULATION

A. Motion capture

1) Motion capture-based ICR measurement: A healthy male volunteer (age: 30 years; mass: 58 kg; height:173 cm) participated in this study. The volunteer sat on the chair, and

978-1-6654-5452-0/22/$31.00 ©2022 IEEE

the full HD camera with a frame rate of 60 fps recorded the open kinematic chain movement of the volunteer's leg. In order to find the ICR, four markers are placed on the foot. A and B markers are on the thigh and C and D markers on the leg, as shown in Fig. 1. To find the ICR of the knee joint, the positions of the markets during full range of motion (0° to 160°) are captured by using image processing. The locations of markers are used to estimate the position of the axis of rotation in sagittal plane [14]. This information is used to calculate the path of ICR that is called, the knee centroid. Ten sets of cycle data were collected during the 53-second. Since each cycle has a different angular velocity, the smoothest data set is selected for further analysis. The connections between markers on the thigh and leg are recorded as AB and CD, respectively. Following that, line AB on the thigh in the world coordinate system is fixed, and the position of the CD is corrected. In order to reduce the error of raw data, the statistics moving average method is used. Finally, the ICR path is calculated as shown in Fig. 2 and the coordinates of the knee ICR are reported in Table I.

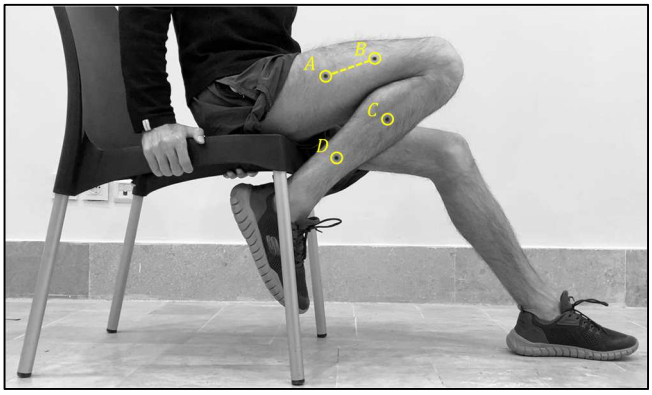

Fig. 1. Motion capture markers

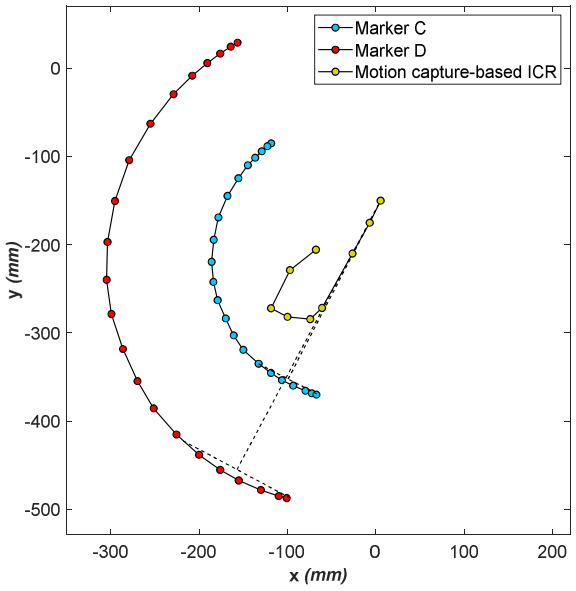

Fig. 2. The motion capture-based ICR of the knee joint

TABLE I. THE COORDINATES OF THE KNEE ICR

#	x (mm)	y (mm)	#	x (mm)	y (mm)
1	5.54	-150.13	6	-99.89	-281.79
2	-6.84	-175.12	7	-118.51	-272.01
3	-26.3	-210.06	8	-97.23	-228.73
4	-60.76	-271.69	9	-67.67	-205.64
5	-74.07	-284.39			

2) Full lunge exercise kinematics parameters measurement: Full lunge kinematic parameters are required as input to solve the dynamic equations of motion, so a CNN-based motion capture method has been used to find the knee angle and the knee angular velocity. In this method, the change of the knee angle is captured with the full HD camera with a frame rate of 240 fps. Seven sets of cycle data were collected during the 36-second. Since each cycle has a different angular velocity, the smoothest data set is selected for further analysis. Fig. 3 shows the full lunge movment and the collected data are shown in Fig. 4.

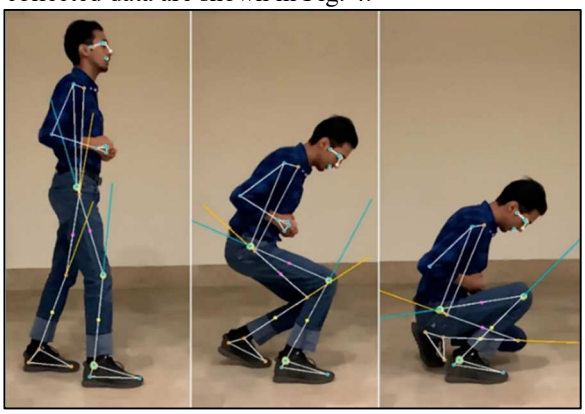

Fig. 3. Full lunge movement

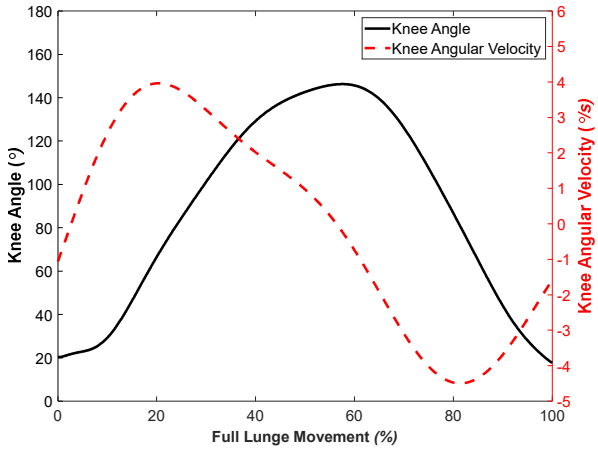

Fig. 4. Full lunge knee angle and knee angular velocity

B. Physiological ICR measurement

In this study, before the data acquisition, as part of the informed consent process, the subject provided written consent for the experiment. The x-ray images are collected by a medical imaging system (Artis zee; Siemens medical solution, USA, Malvern). This operation is done in such a way that the volunteer moves his leg in an open kinematic chain movement loop. The fluoroscopy images were taken

with a rate of 15 fps from the Femur and Tibia bones of the right knee. By using the image processing and edge detection algorithms in Python, four markers E, F, G, and H are calculated and shown in Fig. 5. These four points are next used and the physiological centroid is calculated as shown Fig. 6. The coordinates of the physiological ICR are reported in Table II. In order to reduce the error of the raw data, the statistics moving average method is used.

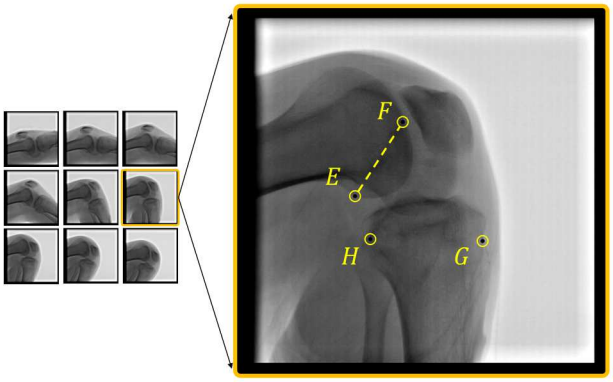

Fig. 5. Fluoroscopy open kinematic chain images

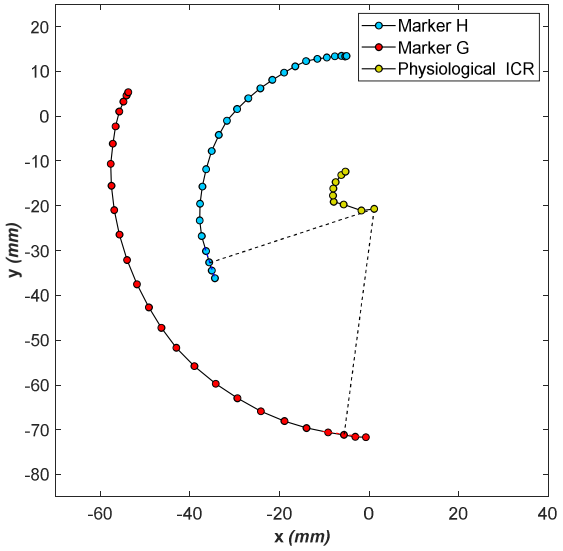

Fig. 6. The physiological ICR of the knee joint

TABLE II. THE COORDINATES OF THE PHYSIOLOGICAL ICR

#	x (mm)	y (mm)	#	x (mm)	y (mm)
1	1.14	-20.67	6	-8.00	-16.14
2	-1.72	-21.04	7	-7.47	-14.69
3	-5.68	-19.70	8	-6.21	-13.13
4	-7.90	-19.09	9	-5.27	-12.35
5	-8.06	-17.70			

III. OPTIMIZATION

In this paper, two different methods are used to obtain the instantaneous center of knee rotation. After obtaining the data of motion capture and fluoroscopy methods, the ICRs of these two imaging systems are given as input to kinematic optimization. After that, the most suitable elliptical curves are obtained for each ICRs. Then, the average scale between these optimized elliptical curves is taken, and the "combined pitch curve" is created. The combined pitch curve is used to form the ICR of the knee joint in the NGF mechanism. To obtain the best design parameters, the combined pitch curve and the kinematic parameters of the knee joint during full lunge movement are given as input to the dynamic optimization.

A. Kinematics optimization

An elliptic curve is one of the closest curves to the J-shaped ICR of the knee. The ICR path creates a space cone on the global coordinate system and a body cone on the moving body that these two cones roll on each other [15]. By using this theory, the elliptical pitch curve is used to design an elliptical gear which is considered as the space cone. The shape and parameters of the corresponding training gear, considered as the body cone, is next calculated using the non-circular gears design approach [16]. The rolling of these two pitch curves makes the ICR of the knee mechanism. As shown in Fig. 8, a and b are the kinematics optimization parameters and l_{cg} is calculated from non-circular gears design approach [16].

As shown the kinematic optimization parameters in Fig. 7. Since the ICR of the knee is J-shaped, an elliptical curve is selected to be considered as the pitch curve. By considering the a_j and b_j as the semi-major and semi-minor axes of this ellipse, the goal of the cost function will be finding the best fit elliptical curve on the path of ICRs. The full factorial design of experiment is performed and the cost function (1) is defined. a_j and b_j are the constraints which are searched by the optimization algorithm.

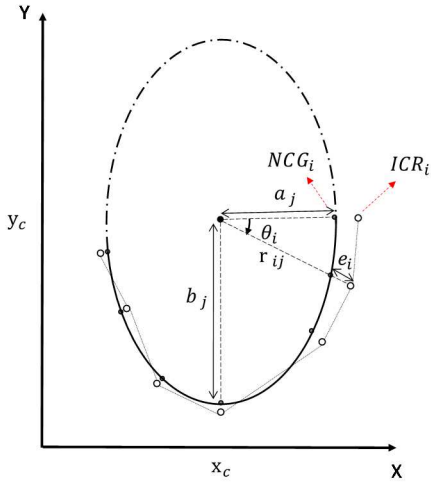

Fig. 7. The schematic of kinematic optimization parameters

$$COST_{kin} = \sum_{i=1}^{n} \sqrt{(y_{ICR_i} - y_{NCG_i})^2 + (x_{ICR_i} - x_{NCG_i})^2}\ ,\ i = 1,2,...,n \qquad (1)$$

Where x_{NCG_i} and y_{NCG_i} are the coordinates on the ellipse perimeter, the x_{ICR_i} and y_{ICR_i} are the coordinates of ICR points and i indicates the i-th ICR point. The cost function finds the sum of each error distance e_i of the corresponding ellipse perimeter points with respect to the corresponding ICR points. The optimal values result in minimize the cost function.

$$\begin{cases} x_{NCG_i} = r_{ij} \cos\theta_i \\ y_{NCG_i} = r_{ij} \sin\theta_i \end{cases} \qquad (2)$$

$$\theta_i = \text{atan}\,2(y_{ICR_i} - y_c, x_{ICR_i} - x_c) \tag{3}$$

$$r_{ij} = \frac{a_j b_j}{\sqrt{a_j^2 \sin^2\theta_i + b_j^2 \cos^2\theta_i}} \tag{4}$$

Where r_{ij} is the ellipse radius which is obtained from θ_i.

B. Dynamics optimization

1) System dynamics: NGF mechanism provides one degree of freedom. This mechanism comprises of a four-bar mechanism and a pair of non-circular gears. The four-bar mechanism includes links l_0, l_1, l_2 and l_3 in which l_1, l_2 and l_3 are the dynamic parameters. The actuator is located in approximate to the thigh center of mass to mitigate distal mass distribution to decrease the metabolic cost burden [3]. l_0 is the distance between the the thigh center of mass and the knee joint that is calculated according to the method presented in [17]. The pitch curves for the two non-circular gears, represented as the space cone and the body cone, are named SG and BG, respectively. As shown in Fig. 9, for simplification, the total weight and inertia of a human foot and leg is modelled as circle with similar weight and inertia. BG then connects link l_4 to this circle. In the dynamics optimization, the weight of the volunteer leg is calculated [17]. The SG and BG gears are connected by a triangular-shaped body. The sides of this body consist of l_{cg}, which connects the centers of the non-circular gears to each other, and the other side is l_3, which plays a role as the last link of the four-bar mechanism. The angle between l_3 and l_{cg} is called ν, and is considered as the last dynamic optimization parameters. The kinematics parameters are solved according to (5) and (6), which represent the closed-loop equation of the four-bar mechanism. The relation of the velocities between the SG and BG gears is defined by (7).

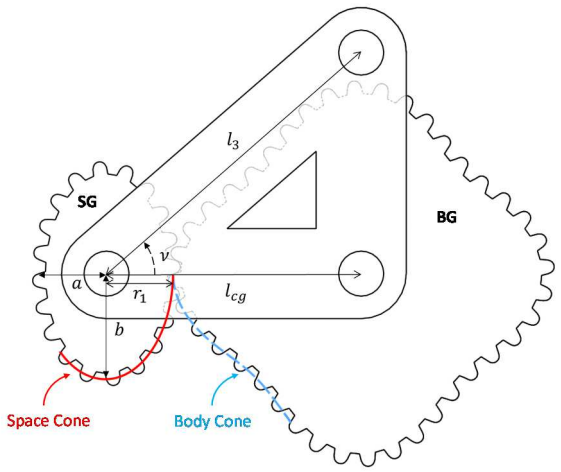

Fig. 8. The schematic of the non-circular gears and the triangular-shaped body

$$-l_1\cos\theta - l_2\cos\alpha + l_3\cos\phi = 0 \tag{5}$$

$$-l_1\sin\theta - l_2\sin\alpha - l_0 + l_3\sin\phi = 0 \tag{6}$$

$$\dot{\psi} = \frac{l_{cg}}{l_{cg} - r_1}\dot{\phi} \tag{7}$$

Where l_{cg} is the distance between gear centers and r_1 is the distance between the SG center and the gears' pitch contact point defined by (8).

$$r_1 = \frac{ab}{\sqrt{a^2\sin^2\phi + b^2\cos^2\phi}} \tag{8}$$

The dynamics of this system is a Lagrange equation with non-holonomic constraints. There are two generalized coordinates in this model so by using one velocity constraint equation (13) and the Lagrange multiplier λ, the equation of motion (12) has been solved.

$$L = T - V \tag{9}$$

$$T = \sum_{i=1}^{n} T_i,\ i = 1,2,...,n \tag{10}$$

$$V = \sum_{i=1}^{n} V_i,\ i = 1,2,...,n \tag{11}$$

The Lagrangian of the entire system is defined as (9) Where T_i and V_i correspond to the kinetic and potential energy of each link.

$$\frac{d}{dt}\left(\frac{\delta L}{\delta\dot{\theta}}\right) - \frac{\delta L}{\delta\theta} = \tau_\theta + \frac{l_{cg} l_1 \sin(\alpha-\theta)}{(l_{cg} - r_1) l_3 \sin(\alpha-\phi)}\lambda$$
$$\frac{d}{dt}\left(\frac{\delta L}{\delta\dot{\psi}}\right) - \frac{\delta L}{\delta\psi} = \lambda \tag{12}$$

$$\frac{l_{cg} l_1 \sin(\alpha-\theta)}{(l_{cg} - r_1) l_3 \sin(\alpha-\phi)}\dot{\theta} + \dot{\psi} = 0 \tag{13}$$

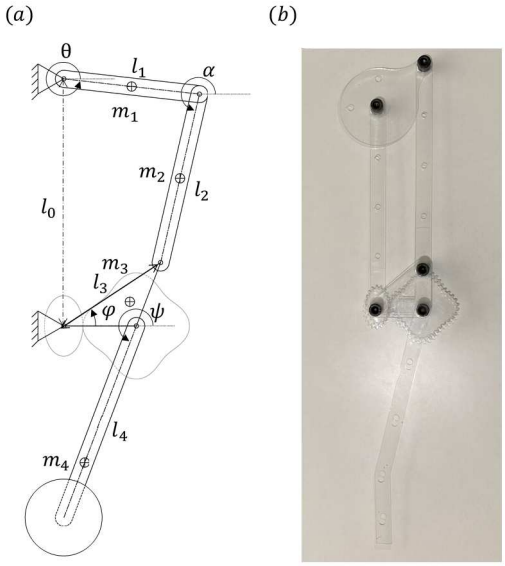

Fig. 9. The schematic diagram (a) and the prototype (b) of the mechanism

2) Cost function: To get the most optimal mechanism regarding the best performance during our scenario (full lunge movement), the full factorial designed experiments are performed and the cost function is (14). To obtain optimal dynamics values, the values of the trial that has the minimum value of (14) are selected. This optimization results in a lower weight and minimum range of actuator torque to apply the required force.

$$COST_{dyn} = K_1(\frac{m_i}{m_{\max}}) + K_2(\frac{\tau_i}{\tau_{\max}}),\ i = 1,2,...,n \qquad (14)$$

Where $K_1 = 0.8$ and $K_2 = 0.2$ are the factor of each goal of the multi-objective cost function. m and m_{max} are the total mechanism mass and maximum mechanism mass obtained by constraints. τ and $\tau_{\max}$ are the maximum actuator torque in each cycle and rated torque value of the selected motor (T-motor AK10-9 V2.0) respectively.

IV. Resualt and Descussion

The results of the kinematic optimization are shown in Fig. 10 and Fig. 11. The sizes of the physiological and knee ICRs are vastly different [13]. Leg muscles and their tissues have Ogden hyperelastic model properties [18]; therefore, changes in muscle volume are observed in the knee's range of motion. So, this issue may be the reason for the vast difference between the ICR observed in the motion capture method from the ICR of the knee bones calculated using fluoroscopy. By using the average scale between these optimized elliptical curves, the combined pitch curve is selected to be the pitch curve of the designed space cone gear, as shown in Fig. 12. The kinematics optimized values of a and b for the combined pitch curve and its corresponding calculated l_{cg} are reported in Table III. In our dynamic model, for the full lunge movement, the optimal torque was obtained in the range of $\pm 10\ (N.m)$, as shown in Fig. 13 and the dynamics optimized design parameters are reported in Table IV.

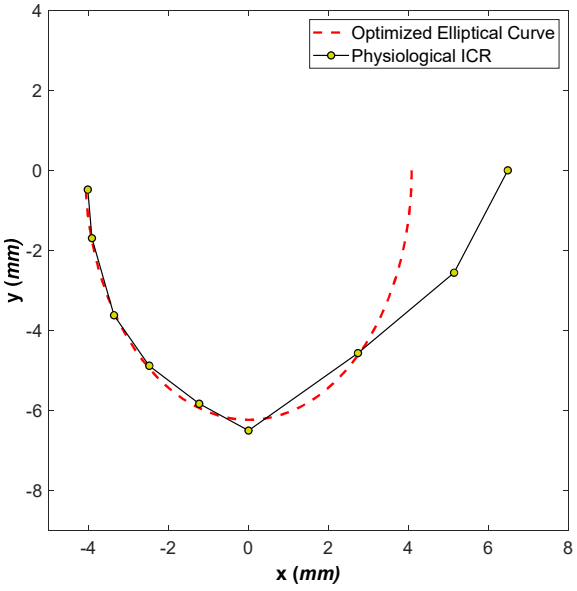

Fig. 10. Comparsion between the physiological ICR and the optimized elliptical curve for the fluroscopy approach

TABLE III. The Final Kinematics Optimized Designed Parameters

parameters	a(mm)	b(mm)	l_{cg}(mm)
optimal results	29.32	92.56	157.94

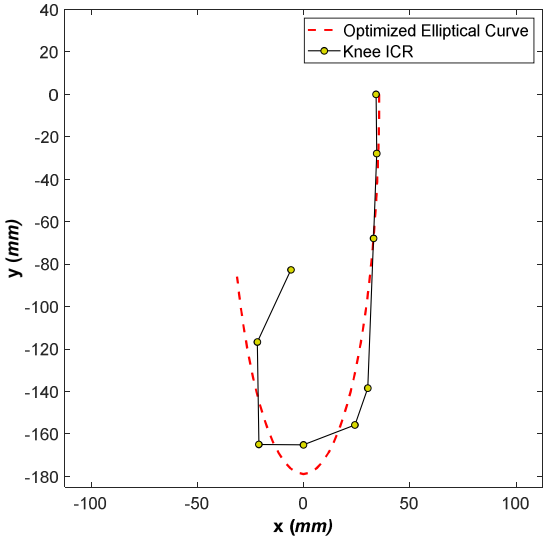

Fig. 11. Comparsion between the knee ICR and the optimized elliptical curve for the motion capture approach

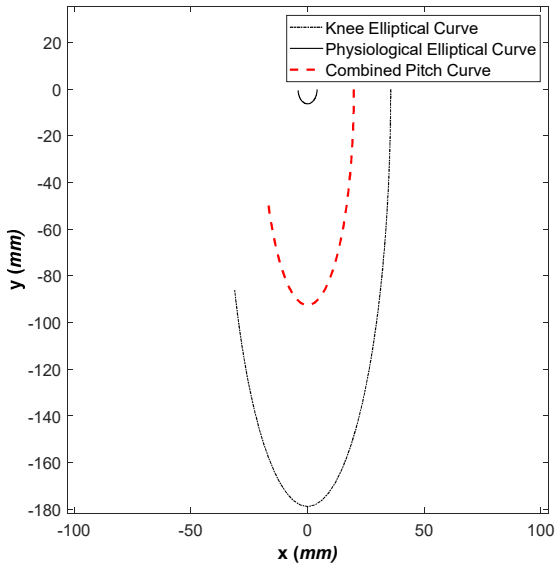

Fig. 12. Combined pitch curve of the designed space cone gear

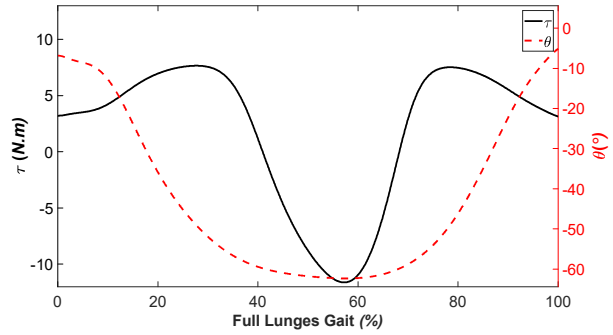

Fig. 13. The final torque and angle of the motor in range of full lunge movments

TABLE IV. THE FINAL DYNAMICS OPTIMIZED DESIGNED PARAMETERS

parameters	l_1(cm)	l_2(cm)	l_3(cm)	ν(°)
Lower boundary	5	20	5	0
Upper boundary	15	30	15	60
optimal results	6.11	25.55	5	12.63

Nowadays, various mechanisms are developed to follow the instantaneous center of knee rotation. In the following, the advantages and disadvantages of each of these mechanisms are compared with the NGF mechanism. A large number of studies use the four-bar mechanisms. Besides the four-bar mechanism, other multi-bar mechanisms and non-circular gear mechanisms are begging to be used. These mechanisms contain more design parameters than the four-bar mechanism. This provides better bionic knee performance [4]. In [12], circular gears are used to follow the instantaneous center of rotation during movement by the mechanism. Since the ICR is a J-shaped curve, it is better to use an elliptical curve that is more similar to a J-shaped curve; therefore, the path of the ICR of the knee can be better tracked by the NGF mechanism. In the majority of studies, 120° of knee flexion are considered [19] and [7]. However, in order to fully follow the ICR of the knee by the mechanism, it is necessary to follow the ICR up to 150° [20]. The proposed NGF mechanism is designed with this in mind so that it can fully follow the ICR of the knee.

V. CONCLUSION

During open kinematic chain movement, due to the different material behavior of leg muscle tissue compared to the knee bones, two ICRs with entirely different dimensions are exist. This paper considered the two ICRs of the human knee joint, measured using fluoroscopy and motion capture approach from a healthy volunteer. Then, with a kinematic view, the two ICRs tracking error was minimized to obtain the best-fitted elliptical curve for each ICRs. By employing these two ICRs curves, the combined pitch curve was calculated to create a pair of non-circular gears. This resulted in the best kinematics solution for tracking the path of ICR. As a result, the robot's slipping on the body is minimized during motion. Next, a dynamics approach with the full lunge movement as input was used. This resulted in parameters that minimized actuator torque and mechanism weight. The proposed approach increases the mechanism's efficiency and subsequently reduces the battery consumption enabling smaller and less expensive motors and batteries.

In future works, the effect of the different scales of elliptical curves will be considered to provide a more suitable ICR for this mechanism. Also, the different dynamic models and scenarios for this mechanism will be investigated.

ACKNOWLEDGMENT

This research is supported by Ferdowsi University of Mashhad-Iran under the grant number 101120 and National Institute for Medical Research Development of Iran (NIMAD) under the grant number 962297 and Imam Reza hospital CAT lab center.

REFERENCES

[1] T. R. Marya SKS, *Knee Replacement*. Jaypee Brothers Medical Publishers, 2014.
[2] X. Tang and L. Chen, "Structural design of a novel wearable knee exoskeleton," in *2018 8th International Conference on Manufacturing Science and Engineering (ICMSE 2018)*, 2018: Atlantis Press, pp. 348-353.
[3] J. Wang *et al.*, "Comfort-centered design of a lightweight and backdrivable knee exoskeleton," *IEEE Robotics and Automation Letters,* vol. 3, no. 4, pp. 4265-4272, 2018.
[4] Y. Sun *et al.*, "Review of Recent Progress in Robotic Knee Prosthesis Related Techniques: Structure, Actuation and Control," *Journal of Bionic Engineering,* vol. 18, no. 4, pp. 764-785, 2021.
[5] J. W. Bneakey and S. H. Marquette, "Beyond the four-bar knee," *JPO: Journal of Prosthetics and Orthotics,* vol. 10, no. 3, pp. 77-80, 1998.
[6] R. Singh, H. Chaudhary, and A. K. Singh, "Defect-free optimal synthesis of crank-rocker linkage using nature-inspired optimization algorithms," *Mechanism and Machine Theory,* vol. 116, pp. 105-122, 2017.
[7] M. Gao *et al.*, "Design and optimization of exoskeleton structure of lower limb knee joint based on cross four-bar linkage," *AIP Advances,* vol. 11, no. 6, p. 065124, 2021.
[8] D. J. Hyun, H. Park, T. Ha, S. Park, and K. Jung, "Biomechanical design of an agile, electricity-powered lower-limb exoskeleton for weight-bearing assistance," *Robotics and Autonomous Systems,* vol. 95, pp. 181-195, 2017.
[9] B. Xiao, Y. Shao, and W. Zhang, "Design and optimization of single-degree-of-freedom six-bar mechanisms for knee joint of lower extremity exoskeleton robot," in *2019 IEEE International Conference on Robotics and Biomimetics (ROBIO)*, 2019: IEEE, pp. 2861-2866.
[10] J. Choo and J. H. Park, "Increasing payload capacity of wearable robots using linear actuators," *IEEE/ASME Transactions on Mechatronics,* vol. 22, no. 4, pp. 1663-1673, 2017.
[11] A. H. Slocum, D. Goodman, M. Eilenberg, J. Titarelli, and L. Meyer, "Rolling-contact knee prosthesis," ed: Google Patents, 2014.
[12] Y. Sun, W. Ge, J. Zheng, and D. Dong, "Design and evaluation of a prosthetic knee joint using the geared five-bar mechanism," *IEEE Transactions on Neural Systems and Rehabilitation Engineering,* vol. 23, no. 6, pp. 1031-1038, 2015.
[13] S. Pfeifer, R. Riener, and H. Vallery, "An actuated transfemoral prosthesis with optimized polycentric knee joint," in *2012 4th IEEE RAS & EMBS International Conference on Biomedical Robotics and Biomechatronics (BioRob)*, 2012: IEEE, pp. 1807-1812.
[14] D. A. Neumann, E. R. Kelly, C. L. Kiefer, K. Martens, and C. M. Grosz, *Kinesiology of the Musculoskeletal System: Foundations for Rehabilitation*. Elsevier, 2017.
[15] J. L. Meriam and L. G. Kraige, *Engineering Mechanics: Dynamics*. Wiley, 2012.
[16] I. Zarębski and T. Sałaciński, "Designing of non-circular gears," *Archive of Mechanical Engineering,* pp. 275-292-275-292, 2008.
[17] C. L. Vaughan, *Dynamics of Human Gait*. Human Kinetics Books, 1992, pp. 2-3.
[18] S. Kallin, A. Rashid, K. Salomonsson, and P. Hansbo, "Comparison of mechanical conditions in a lower leg model with 5 or 6 tissue types while exposed to prosthetic sockets applying finite element analysis," *arXiv preprint arXiv:1907.13340,* 2019.
[19] M. R. Tucker, A. Moser, O. Lambercy, J. Sulzer, and R. Gassert, "Design of a wearable perturbator for human knee impedance estimation during gait," in *2013 IEEE 13th International Conference on Rehabilitation Robotics (ICORR)*, 2013: IEEE, pp. 1-6.
[20] B. Tillman, P. Tillman, and W. Woodson, *Human Factors Design Handbook*. McGraw-Hill Education, 1992.